

Optical-absorption coefficient of $\text{In}_{1-x}\text{Ga}_x\text{As}/\text{InP}$

F. R. Bacher and J. S. Blakemore

Department of Applied Physics and Electrical Engineering, Oregon Graduate Center, Beaverton, Oregon 97006-1999

J. T. Ebner and J. R. Arthur

Department of Electrical and Computer Engineering, Oregon State University, Corvallis, Oregon 97331-3202

(Received 17 July 1987)

Optical-absorption coefficient data are presented over the 0.7–1.5-eV spectral range (825–1750 nm) for $\text{In}_{1-x}\text{Ga}_x\text{As}/\text{InP}$; both at the lattice-matched condition $x=0.47$ and for the $0.45 < x < 0.51$ composition range. Absorption data for such epilayers are compared at 10, 77, and 300 K. This comparison involves numerous epilayers grown by organometallic vapor-phase epitaxy, a lattice-matched layer grown by molecular-beam epitaxy, and published data for $\text{In}_{1-x}\text{Ga}_x\text{As}$ grown by liquid-phase epitaxy. It is demonstrated that these growth techniques yield material with equivalent absorption characteristics. For all compositions, the absorption coefficient $\alpha(h\nu)$ rises abruptly to near 6000 cm^{-1} at the band gap, and increases more gradually to 30000 cm^{-1} at 1.5 eV. For energies above 1.3 eV, all the $\text{In}_{1-x}\text{Ga}_x\text{As}$ epilayers studied here show essentially the same absorption characteristics, regardless of composition or temperature.

I. INTRODUCTION

Extensive literature since the 1970s attests to a developing interest in the $\text{In}_{1-x}\text{Ga}_x\text{P}_{1-y}\text{As}_y$ quaternary system, which can be epitaxially grown matched to the 5.87-Å lattice constant of InP when $y \approx 2.1x$. In this paper we report on intrinsic optical absorption for the ternary $\text{In}_{1-x}\text{Ga}_x\text{As}$ (i.e., for $y=0$), for a number of epitaxial samples at the $x=0.47$ lattice-matched composition, and also for an [In]:[Ga] ratio range straddling that composition which matches the lattice constant of an InP substrate.

Despite considerable interest in $\text{In}_{1-x}\text{Ga}_x\text{As}$ for optoelectronic applications, quantitative data of the optical-absorption coefficient $\alpha(h\nu)$ near and above band gap are scanty.^{1,2} Some other accounts have quoted α in “arbitrary units” only. Since α is one of the principal optical properties for $\text{In}_{1-x}\text{Ga}_x\text{As}$, we have measured $\alpha(h\nu)$ for a number of ternary samples, in the range 10–300 K, and report these data here.

The above-noted reports^{1,2} of intrinsic absorption for $\text{In}_{1-x}\text{Ga}_x\text{As}$ comprise data from layers grown by liquid-phase epitaxy (LPE). We present here quantitative absorption results over a broad spectral range for $\text{In}_{1-x}\text{Ga}_x\text{As}$ grown by organometallic vapor-phase epitaxy (OMPVE) and by molecular-beam epitaxy (MBE), at both cryogenic and room temperatures. Further, we give $\alpha(h\nu)$ data for varying compositions of $\text{In}_{1-x}\text{Ga}_x\text{As}$ not lattice-matched to InP (i.e., $x \neq 0.47$). These data are then compared with the reported work^{1,2} for LPE-grown $\text{In}_{0.53}\text{Ga}_{0.47}\text{As}$.

Among the steps taken by us to achieve maximum precision in the deduction of $\alpha(h\nu)$ may be noted the allowance we make for the temperature and spectral dependences of the $\text{In}_{1-x}\text{Ga}_x\text{As}$ refractive index. That affects making proper allowance for reflection losses in

transmittance measurement, and is also required for accurate interferometric determination of an epilayer's thickness.

II. EXPERIMENTAL METHODS

A. Sample preparation

1. OMPVE growth

The principles of OMPVE growth for III-V materials have been reviewed elsewhere.³ The technique consists of combining organometallic compounds and hydrides (in the gas phase) at the surface of a heated single-crystal substrate within a (cold-wall) reaction tube. The OMPVE samples for the present work were all grown at the Oregon Graduate Center, the growth made at atmospheric pressure in a horizontal tube OMPVE reactor built by Crystal Specialties, Inc. The reaction tube was of rectangular cross section, $24 \times 40\text{ mm}^2$.

A SiC-coated graphite susceptor held each substrate, inclined at a 10° angle, and was heated by rf induction to 600°C . Hydrogen was used as a carrier gas, at a rate of 4 l/min. The sources used were arsine (from Phoenix Research), trimethylgallium (TMGa) at -9.7°C , and trimethylindium (TMIn) at $+17^\circ\text{C}$. (The latter two were from Alfa Products.)

The [V]/[III] ratio was maintained at 55:1 for all samples, and an arsine overpressure was maintained during cooling. An InP buffer layer was grown under the $\text{In}_{1-x}\text{Ga}_x\text{As}$, but PH_3 was flushed from the reactor prior to ternary growth.

InP substrates were used with $(100) \xrightarrow{2^\circ} (110)$ orientation, and were etched in a 5:1:1 solution of $\text{H}_2\text{SO}_4:\text{H}_2\text{O}_2:\text{H}_2\text{O}$ prior to epilayer growth. Most of the substrates used for optical studies were n -type doped

(InP:S from Sumitomo Electric), and a few were semi-insulating (InP:Fe from ICI Americas). More typically, semi-insulating substrates were used in growing ternary samples for conductivity and Hall-effect analysis.

The OMVPE growth rate was ≈ 1 nm/s, providing a ternary layer ~ 2 μm thick in a time of 30–35 min. The ternary was grown over an InP buffer layer 0.3 μm thick. The epilayer morphology was observed visually and microscopically.

In order to obtain ternary compositions of adjusted [In]:[Ga] ratio, the TMGa source bath temperature was varied while maintaining a constant H_2 flow, thus varying the TMGa vapor pressure in the bubbler. This was done because the source refrigerator temperature control afforded us more sensitivity than would be possible using commercially available mass flow controllers. The composition x of $\text{In}_{1-x}\text{Ga}_x\text{As}$ was determined from both absorption-coefficient and photoluminescence data, and was confirmed by Auger electron spectroscopy.

The mole fraction of TMIn was maintained at 9.25×10^{-5} for all the OMVPE samples. We found that (for our OMVPE system) a [TMIn]/[TMGa] ratio of 2.07:1 was required for ternary epitaxial growth lattice-matched to InP ($x=0.47$). This value of [TMIn]/[TMGa] is in excess of that predicted by stoichiometric considerations, due to the well-known, parasitic reaction of TMIn and AsH_3 prior to the growth zone.³ The depletion of TMIn by this parasitic reaction varied with the [TMIn]/[TMGa] ratio.

2. MBE growth

The MBE growth of $\text{In}_{0.53}\text{Ga}_{0.47}\text{As}$ onto InP substrates was carried out in a Perkin-Elmer 425B system. Each substrate was cleaned *in situ* by heating in the growth chamber, using an incident As_2 beam in order to prevent loss of III-V element. The metal beam fluxes were determined from calculated growth rates, measured by the period of oscillations in the intensity of the reflection electron-diffraction (RED) beams with calibration samples.⁴ The growth rate of the ternary material itself on the InP substrate was measured by the same method. We have previously shown that the [In]:[Ga] ratio can be determined to $\leq 1\%$ by this method, provided that the substrate temperature is maintained below 500°C during growth, in order to avoid loss of indium.⁵

The MBE samples used in this work (including the sample MB-297 for which data appear in several of the figures which follow) were grown at 495°C, at a total growth rate of 0.1 nm/s. Auger spectra from the surface before and after growth showed no detectable impurities at either interface. Moreover, spectra from the surface following growth were consistent with the composition that had been established by the period of RED oscillations.

3. Preparation for transmittance measurements

In preparing a ternary sample for $\alpha(h\nu)$ measurements, the $\text{In}_{1-x}\text{Ga}_x\text{As}$ layer was sealed to a glass slide by means of a thin layer of transparent epoxy. That

leaves the back surface of the InP substrate uppermost. For all of the $\text{In}_{1-x}\text{Ga}_x\text{As}$ samples to be reported on herein, a 38% HCl solution was used to etch away all of the InP substrate and buffer layer.

It is only fair to remark that the procedure noted above was arrived at following various other and less satisfactory ways of preparing the epilayer for transmittance measurement. The procedure had been optimized prior to work with any of the samples to be reported on in Sec. III.

B. Absorption-coefficient measurement

The experimental arrangement for $\alpha(h\nu)$ measurement was conventional, based on a comparison of a transmittance spectral scan with the sample *in* the optical path, normalized by a scan with the sample *out* of that path. A tungsten-halogen light source was coupled to a Jarrell-Ash monochromator with a wavelength-scanning drive mechanism, and the light output was imaged at normal incidence upon one of the two apertures built into the sample holder of an Air Products "Displex" (closed-cycle) cryostat. The transmitted light was collected, and imaged upon a PbS detector. An electrical signal was obtained using a chopper and lock-in amplifier combination. Since high spectral resolution

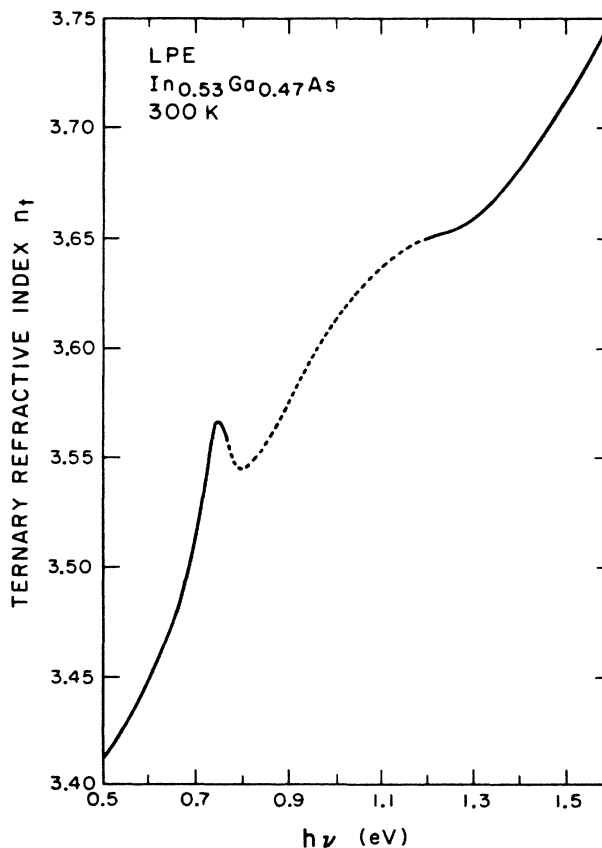


FIG. 1. The spectral dependence of the 300-K refractive index for $\text{In}_{0.53}\text{Ga}_{0.47}\text{As}$, as reported in Ref. 6 for $h\nu < 0.76$ eV, and in Ref. 7 for $h\nu > 1.2$ eV. The dashed curve shows our estimate for intermediate energies.

was secondary in our study of $\alpha(h\nu)$, compared with a primary objective of having an acceptable signal-to-noise ratio when (αt) was as large as 6, our transmittance measurements were usually made with the monochromator slits fairly wide, for a spectral resolution of ~ 4 meV.

The signal S_1 (via aperture no. 1, blocked by the $\text{In}_{1-x}\text{Ga}_x\text{As}$ sample) or S_2 (via aperture no. 2, containing only the bare glass slide) was typically plotted versus wavelength with an analog X - Y recorder. From these raw data, the sample transmittance T is almost—but not quite—equal to S_1/S_2 . One small correction arises from minute differences of aperture areas. (Fine adjustments were always made to maximize the optical throughput when the cryostat was translated to position apertures no. 1 or no. 2 in the light path.) Note that signal S_2 is affected by the cryostat windows, and by reflection losses at front and rear faces of the glass slide. Signal S_1 is similarly affected by the windows, but the light path inside the cryostat must now enter the glass slide, pass through the epoxy and the $\text{In}_{1-x}\text{Ga}_x\text{As}$, and be transmitted at the $\text{In}_{1-x}\text{Ga}_x\text{As}$ -vacuum interface.

In order to convert data of $T(\lambda)$ into $\alpha(h\nu)$, it is necessary to know the refractive indexes of the glass ($n_g=1.5$), the epoxy (n_e), and the ternary (n_t). Only two studies^{6,7} are known to us of the refractive index for $\text{In}_{0.53}\text{Ga}_{0.47}\text{As}$. The data from these, valid for 300 K, are reproduced as the two solid parts of the curve in Fig. 1. Of these, the portion for $h\nu < 0.76$ eV is taken from the work of Chandra *et al.*,⁶ while that for $h\nu > 1.2$ eV comes from Burkhard *et al.*⁷ The dashed part of the

curve shows our attempt at interpolation, in order to yield an acceptable estimate of n_t over the spectral range of concern to us, as needed both for interferometric thickness measurement and for calculation of the reflectivities R_{vt} and R_{et} of vacuum-ternary and epoxy-ternary interfaces.

For calculation of $n_t(h\nu)$ at 77 or 10 K, the data of Fig. 1 were shifted towards higher energy by 40 or 60 meV, respectively, to correspond with the variation of band gap with temperature. We did not attempt to estimate any variation of the n_t behavior with changing ternary composition x .

As for the other transmitting media, we assumed a glass refractive index $n_g=1.5$ for all wavelengths and temperatures, to provide a vacuum-glass reflectivity $R_{vg}=0.04$. Thus $1-R_{vg}=0.96$, a factor appearing in the denominators of Eqs. (1) and (4). The index n_e of the epoxy was measured by comparing the transmission of an epoxy layer sandwiched between two glass slides with that of a pair of identical slides separated by an air gap. From this we concluded that $n_e \simeq 1.30$ for this epoxy, at cryogenic and room temperatures, over the near-ir range.

In calculating α , we used an equation derived by Moss⁸ for the transmittance of a partly absorbing layer (of thickness t) when multiply reflected components add coherently. Inserting additional factors arising from our use of the glass slide and epoxy mounting layer, Moss's equation becomes

$$T = \frac{(1-R_{vt})(1-R_{et})(1+k_t^2/n_t^2)}{0.96\{[e^{\alpha t/2} - (R_{vt}R_{et})^{1/2}e^{-\alpha t/2}]^2 + 4(R_{vt}R_{et})^{1/2}\sin^2(\psi + 2\pi t n_t/\lambda)\}} \quad (1)$$

In addition to quantities defined above, here $k_t = \alpha\lambda/4\pi$ is the ternary's extinction coefficient—imaginary part of the complex refractive index. Also,

$$\psi = \arctan [2k_t/(n_t^2 + k_t^2 - 1)] \quad (2)$$

Interference effects were significant in the $T(\lambda)$ data for our thin, highly reflective samples—even though the monochromator was set for a rather modest spectral resolution. Inclusion of the interference effects complicated our analysis, but we were able to use this in making an accurate determination of epilayer thickness. For $h\nu < \epsilon_i$, an $\text{In}_{1-x}\text{Ga}_x\text{As}$ layer with the InP substrate removed functioned as a Fabry-Perot étalon, and a plot of $T(\lambda)$ showed a prominent succession of minima and maxima. The thickness was easily determined, since $t = m\lambda/2n_t$ at normal incidence, where m is the order of

successive maxima. The number m was found by comparing wavelengths for several maxima, using the appropriate value of n_t for each.

Equation (1) can be slightly simplified by noting that $k_t^2 = (\alpha\lambda/4\pi)^2 \ll n_t^2$ even up to the largest values of α ($\sim 30\,000$ cm^{-1}) involved in our study. Moreover, the angle ψ defined in Eq. (2) can be simplified by means of

$$\begin{aligned} \psi &\simeq \arctan [2k_t/(n_t^2 - 1)] \\ &\simeq \arctan [\alpha\lambda/2\pi(n_t^2 - 1)] \\ &\simeq [\alpha\lambda/2\pi(n_t^2 - 1)] \end{aligned} \quad (3)$$

since the argument of the arctangent is always much less than unity.⁹ These considerations permit us to reexpress Eq. (1) in the form

$$T = \frac{(1-R_{vt})(1-R_{et})}{0.96\{e^{\alpha t} + R_{vt}R_{et}e^{-\alpha t} - 2(R_{vt}R_{et})^{1/2}\cos[\alpha\lambda/\pi(n_t^2 - 1) + 4\pi t n_t/\lambda]\}} \quad (4)$$

TABLE I. Estimates of possible error in quantities used for calculation of α .

Parameter	Proportional error
Refractive indexes:	
epoxy, n_e	0.04
ternary, n_t	0.01
glass, n_g	0.01
Optics:	
transmission, T	0.005
wavelength, λ	0.005
scale factor	0.01
Thickness t	0.04

Equation (4) does not provide a unique closed-form solution for α in terms of T and λ , but formed the basis of a computer program we used to obtain α iteratively, to three significant figures. Solutions so obtained were considered reliable within the absorbance range $0.2 < \alpha t < 6.0$.

The proportional error values (all independent and symmetrical with regard to sign) for the various steps in evaluation of α are shown in Table I. Combining these by least squares gives an estimated $\pm 7\%$ total uncertainty in our deduced values for α .

C. Supplemental measurements

These $\text{In}_{1-x}\text{Ga}_x\text{As}$ samples were usually examined by photoluminescence (PL) before removal of the InP substrate, using an experimental arrangement that has been described elsewhere.¹⁰ Data of electrical conductivity and Hall effect were obtained using the van der Pauw technique.¹¹ Ohmic indium contacts for that purpose were annealed in argon for 30 sec at 200°C.

Representative OMVPE and MBE samples were subjected to compositional analysis at the facilities of Charles Evans and Associates, using Auger electron spectroscopy and secondary ion mass spectroscopy. The results from those analyses helped confirm the compositions established from optical-absorption and PL data.

III. RESULTS AND DISCUSSION

A. For lattice-matched $\text{In}_{1-x}\text{Ga}_x\text{As}/\text{InP}$

1. Low-temperature data

It will be remembered that lattice matching to an InP substrate connotes that $x = 0.47$ in $\text{In}_{1-x}\text{Ga}_x\text{As}$. Figure 2 shows $\alpha(h\nu)$ data at our lowest temperature (≈ 10 K) for an OMVPE sample (OM-65) and a MBE sample (MB-297) of this composition. For comparison, the curve in Fig. 1 shows ~ 5 -K data reported by Zielinski *et al.*¹ for a LPE-grown sample of the same composition. Note that sample OM-65 has a $h\nu \approx \epsilon_i$ absorption maximum of ~ 5800 cm^{-1} , in good agreement with that prior work.

One distinction between our analysis and that of Ref. 1 should be noted. Both have modeled the steep rise of α at the intrinsic threshold by the Elliott model¹² for the

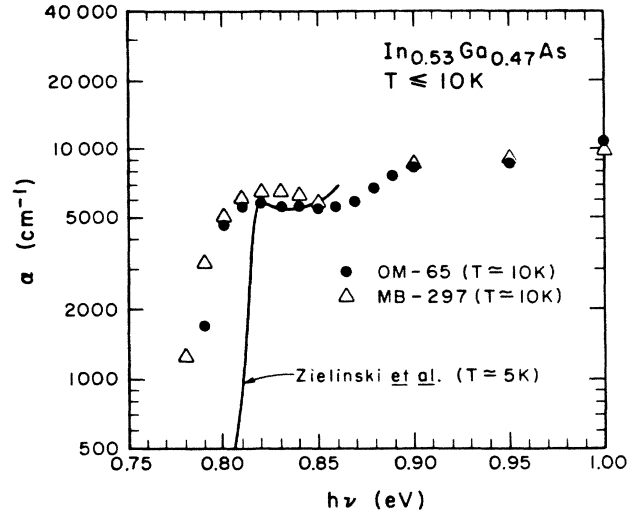


FIG. 2. Low-temperature ($T \leq 10$ K) optical data for $\text{In}_{1-x}\text{Ga}_x\text{As}$ lattice-matched to the InP growth substrate, with examples of three epilayer growth techniques. The solid line is for the LPE sample reported in Ref. 1 by Zielinski *et al.*

electron-hole Coulomb interaction. Zielinski *et al.* concluded thereby that $\epsilon_{i0} = 0.82$ eV, whereas we find $\epsilon_{i0} = 0.81$ eV to fit better for the lowest-temperature absorption data. Our value is supported by the observations of Kuo *et al.*,¹³ and by deductions of Goetz *et al.*¹⁴ from exciton PL measurements at 2 K.

Figure 3 shows $\alpha(h\nu)$ data taken at 77 K for the same two samples as in Fig. 2, grown by OMVPE and MBE, respectively, to achieve the InP lattice-match condition ($x = 0.47$). As expected, the edge has shifted slightly towards lower energy, but the $\alpha(h\nu)$ characteristic is otherwise not markedly different from that at ≈ 10 K. Data from other sources do not appear to be available for comparison with our own at 77 K, for this temperature was by-passed by Zielinski *et al.*,¹ while the near-threshold data of Goetz *et al.*¹⁴ for 77 K were provided only with an "arbitrary units" ordinate scale.

Since the 77-K data of Fig. 3 and the 300-K data of Fig. 4 both extend upwards to $\alpha \approx 3 \times 10^4$ cm^{-1} for $h\nu \approx 1.5$ eV, this is an appropriate point at which to note that α does not rise above the intrinsic threshold as rapidly in $\text{In}_{1-x}\text{Ga}_x\text{As}$ as it does in either GaAs (Ref. 15) or InP (Ref. 16). The rate of increase is more commensurate with that shown by Dash and Newman¹⁷ for the direct-gap region of germanium, which has (not too surprisingly) a number of band-structure similarities with $\text{In}_{1-x}\text{Ga}_x\text{As}$.

2. Room-temperature data

For $T \approx 300$ K, there are three published sources of quantitative $\alpha(h\nu)$ information, about various parts of the intrinsic absorption region for the lattice-matched $\text{In}_{0.53}\text{Ga}_{0.47}\text{As}$ ternary, that can usefully be incorporated into Fig. 4. In each of those cases, the material was grown by LPE. Proceeding upwards in energy ranges, curve (a) in Fig. 4 shows the 301-K data of Zielinski

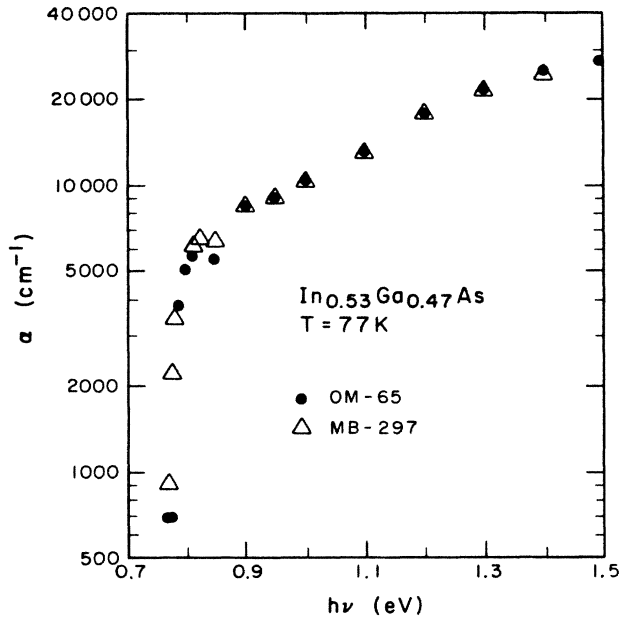


FIG. 3. Optical-absorption 77-K data for the same OMVPE and MBE samples as used in Fig. 2; these grown with $x=0.47$ to be lattice-matched to InP.

et al.,¹ which covered only the range up to 0.8 eV. Curve (b) traces a course through the data for the n^- -doped sample of Humphreys *et al.*,² while curve (c) shows an estimate by Burkhard *et al.*⁷ of α for $h\nu \geq (\epsilon_i + 0.45 \text{ eV})$, derived from ellipsometry measurements which can yield k_t as well as n_t when k_t is not too

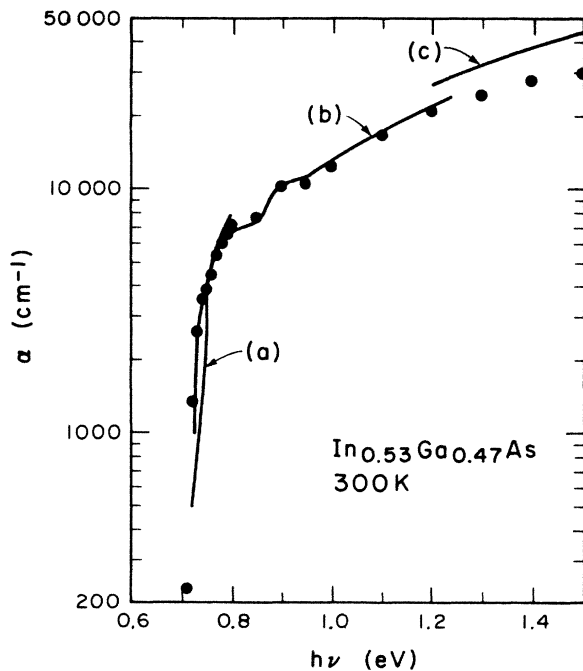


FIG. 4. 300-K absorption-coefficient data for the lattice-matched $x=0.47$ composition. The data points are for the OM-65 and MB-297 samples of Figs. 2 and 3. The curves are (a) after Zielinski *et al.* (Ref. 1), (b) after Humphreys *et al.* (Ref. 2), and (c) after Burkhard *et al.* (Ref. 7).

small.

Those three curves from prior work in Fig. 4 are then combined with data points we measured for $T \approx 300 \text{ K}$, with the samples OM-65 and MB-297 for which lower-temperature data had been shown in Figs. 2 and 3. Our room-temperature data for the OMVPE and MBE samples were essentially coincident, and no distinction is made in Fig. 4 as to which points were measured for one or both of these samples. Over the range shown, at goes from a maximum value of about 6.2 to a minimum of ~ 0.25 , with one fortuitous point at $at \approx 0.05$ just above the baseline.

Omitted by intent from the multisource comparison of room-temperature $\alpha(h\nu)$ data in Fig. 4 is the $\text{In}_{0.53}\text{Ga}_{0.47}\text{As}$ absorption curve of Evtikhiev *et al.*¹⁸ The LPE sample used in that work was noted as having $n_0 \approx 10^{17} \text{ cm}^{-3}$, which should cause a Burstein-Moss shift of the intrinsic edge, and cause other complications outside our area of concern. The nonlinear absorption of $\text{In}_{1-x}\text{Ga}_x\text{As}/\text{InP}$ at room temperature reported by Fox *et al.*¹⁹ from measurements using an intense laser beam also is not pertinent to the present study.

Our data in Fig. 4 using OMVPE and MBE $\text{In}_{0.53}\text{Ga}_{0.47}\text{As}$ samples are in general agreement with those found for LPE-grown material. One would expect this to be so, and confirmation is satisfactory. We find consistently lower values for α than Burkhard *et al.*⁷ in the (high-energy) range, yet remain confident that our measurements of layer thickness and the other quantities pertaining to absolute scaling of α have been under control (cf. Table I).

Neither our data nor those of Humphreys *et al.*² show any perceptible further rise of absorption at the threshold $\epsilon_i + \Delta_0 \approx 1.1 \text{ eV}$ for interband transitions from the split-off valence band.²⁰ However, the lattice-matched OMVPE-MBE samples do show—as does the work of Ref. 2—an appreciable rise in α for $h\nu \approx \epsilon_i + 0.1 \text{ eV}$, for which we have no obvious explanation. As will be noted in Sec. III B, that secondary rise feature was found in some—but not all—layers of OMVPE $\text{In}_{1-x}\text{Ga}_x\text{As}$ for which $x \neq 0.47$.

3. Supplemental data

Brief notes are included here on some other attributes of the $\text{In}_{1-x}\text{Ga}_x\text{As}/\text{InP}$ lattice-matched samples, based on various measurements of a variety of OMVPE and MBE samples with that $x=0.47$ composition. Such samples usually showed good surface morphology, comparable to that of GaAs-on-GaAs epilayers.

The “not intentionally doped” OMVPE material is typically weakly n type, with $n_0 \approx 2 \times 10^{15} \text{ cm}^{-3}$, indicative that there is still room for further materials quality improvement. As of early 1987, the “best” Hall mobility values were $\sim 9000 \text{ cm}^2/\text{Vs}$ at 300 K, and $\sim 27000 \text{ cm}^2/\text{Vs}$ at 77 K.

Photoluminescence spectra obtained at 77 K are shown in Fig. 5 for one of the lattice-matched OMVPE $\text{In}_{1-x}\text{Ga}_x\text{As}$ samples, as well as for three other ternary samples with $x \neq 0.47$. The large subband-gap PL activity even for sample OM-58 shows that this material does

contain defects, a subject to be reported on elsewhere in detail. However, the PL trace for this sample also reveals a band centered at 0.79 eV, with a full width at half maximum (FWHM) of 21 meV. Other lattice-matched OMVPE samples (including OM-65 as portrayed in Figs. 2-4) also showed a small "intrinsic" PL band and a larger subband-gap PL activity, whereas lattice-matched MBE samples such as MB-297 have their PL activity at 77 K dominated by the 0.79-eV band.

B. Results for $\text{In}_{1-x}\text{Ga}_x\text{As}$ not necessarily lattice-matched

Epilayers of $\text{In}_{1-x}\text{Ga}_x\text{As}$ grown by OMVPE onto InP with $x \neq 0.47$ usually had "fair" morphology. Some samples showed a light gray haze, with occasional dark gray spots. The electron mobility in these materials tended to be about half that for $\text{In}_{0.53}\text{Ga}_{0.47}\text{As}$, both at room temperature and lower temperatures. As illustrated by the PL spectra of Fig. 5, variation of x through adjustment of the $[\text{TMI}]/[\text{TMGa}]$ ratio affects the character of the defect-related PL in addition to modifying the band gap.

In addition to sample OM-65 (of Figs. 2-4), absorption-coefficient spectra were measured for ten other OMVPE $\text{In}_{1-x}\text{Ga}_x\text{As}$ samples, including the quartet for which PL data were indicated in Fig. 5; and thus with representation of $x > 0.47$ (gallium-rich, increased ϵ_i) and of $x < 0.47$ (In-rich, decreased ϵ_i). For these

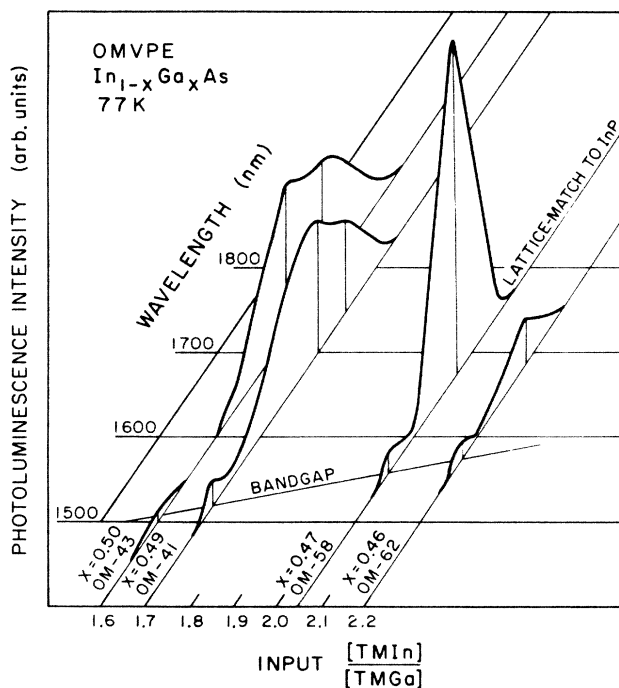


FIG. 5. Schematic of how 77-K photoluminescence of $\text{In}_{1-x}\text{Ga}_x\text{As}$ OMVPE samples progressed with x , changed by adjustment of $[\text{TMI}]/[\text{TMGa}]$ ratio. The change of composition affects the band gap, and also the character of defect-related luminescence.

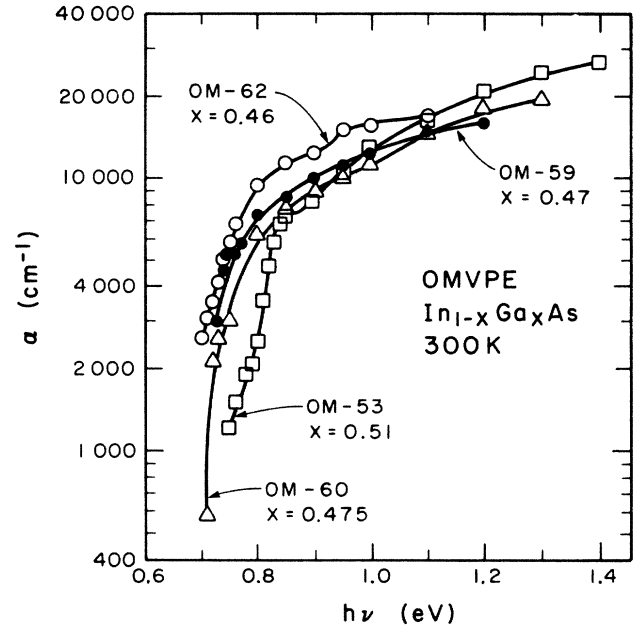


FIG. 6. 300-K absorption data for four OMVPE-grown $\text{In}_{1-x}\text{Ga}_x\text{As}$ samples.

diverse samples, $\alpha(h\nu)$ was measured (after removal of the InP substrates) at $T = 10, 77,$ and 300 K. Examples of the 300- and 10-K data are shown in Figs. 6 and 7, respectively.

Figure 6 exemplifies the room-temperature intrinsic absorption behavior for samples ranging from slightly In-rich to more substantially Ga-rich. The increase of threshold energy is clearly visible for sample OM-53 ($x = 0.51$), and ϵ_i does in fact track properly with x for all four samples. Note that the absorption behavior of the various samples becomes pretty much a communal

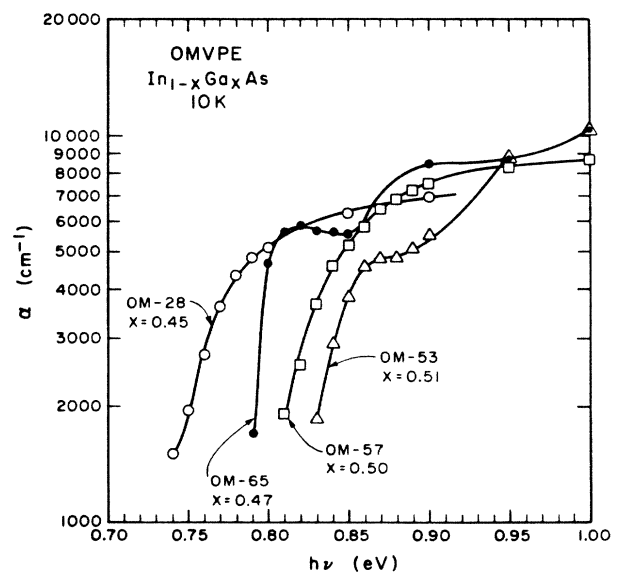


FIG. 7. Absorption-coefficient data at 10 K for four OMVPE-grown $\text{In}_{1-x}\text{Ga}_x\text{As}$ samples. Three of these are different from the samples used in Fig. 6.

property for $h\nu > 1$ eV. None of the samples of Fig. 6 shows any step in α above $\epsilon_i + \Delta_0$, and none shows the step in α near $\epsilon_i + 0.1$ eV which appeared to be characteristic of sample OM-65 for all temperatures.

Low-temperature absorption data provide a more challenging examination of $\text{In}_{1-x}\text{Ga}_x\text{As}$ grown not necessarily lattice-matched to an InP substrate. Even though removal of the substrate by etching removes much of the stress built in by growing at a compositional $x \neq 0.47$, there is residual damage of the epilayer. Thus it is reasonable to expect that the low-temperature optical-absorption edge of such $x \neq 0.47$ material will be affected by (i) a change in ϵ_i resulting from the altered [In]:[Ga] ratio, (ii) a superimposed change of ϵ_i ordained by residual stress, and (iii) a decreased slope for the "Urbach tail" of absorption at $h\nu < \epsilon_i$ also the beneficiary of that stress. These forces can be seen at work in Fig. 7, with 10-K $\alpha(h\nu)$ data for four samples. One of these is lattice-matched OM-65, used here for comparison with one In-rich and two Ga-rich samples. These latter three

show appreciable shifting of the edge and decreased slope in the tail.

Nonetheless, a feature shared in common by these samples, and by the others we have measured (those lattice-matched, and those which were not), is that $\alpha \approx 6000 \text{ cm}^{-1}$ just above threshold, thereafter proceeding more or less steadily upwards towards $\sim 30\,000 \text{ cm}^{-1}$ at $h\nu \sim 1.5$ eV. That statement applies regardless of temperature or compositional x .

ACKNOWLEDGMENTS

This work has been supported in part by Tektronix, Inc. and the Tektronix Foundation, and in part by the National Science Foundation through Grant No. DMR-87-00432. The authors wish to thank W. B. Leigh for some useful insights and discussions, and G. Howard for assistance with OMVPE growth. The encouragement of H. Anderton and J. Sachitano is much appreciated.

-
- ¹E. Zielinski, H. Schweizer, K. Struebel, H. Eisele, and G. Weimann, *J. Appl. Phys.* **59**, 2196 (1986).
- ²D. A. Humphreys, R. J. King, D. Jenkins, and A. J. Mosely, *Electron. Lett.* **21**, 1187 (1985).
- ³M. J. Ludowise, *J. Appl. Phys.* **58**, R31 (1985).
- ⁴P. R. Pukite, J. M. Van Hove, and P. I. Cohen, *J. Vac. Sci. Technol. B* **2**, 243 (1984).
- ⁵J. T. Ebner and J. R. Arthur, *J. Vac. Sci. Technol. A* **5**, 2007 (1987).
- ⁶P. Chandra, L. A. Coldren, and K. E. Strege, *Electron. Lett.* **17**, 6 (1981).
- ⁷H. Burkhard, H. W. Dinges, and E. Kuphal, *J. Appl. Phys.* **53**, 655 (1982).
- ⁸T. S. Moss, *Optical Properties of Semiconductors* (Academic, New York, 1959), p. 13.
- ⁹*Handbook of Mathematical Functions*, edited by M. Abramowitz and I. Stegun (National Bureau of Standards, Washington, 1972), p. 81.
- ¹⁰F. R. Bacher and W. B. Leigh, *J. Cryst. Growth* **80**, 456 (1987).
- ¹¹L. J. van der Pauw, *Philips Res. Rep.* **13**, 1 (1958).
- ¹²R. J. Elliott, *Phys. Rev.* **108**, 1384 (1957).
- ¹³C. P. Kuo, S. K. Vong, R. M. Cohen, and G. B. Stringfellow, *J. Appl. Phys.* **57**, 5428 (1985).
- ¹⁴K.-H. Goetz, D. Bimberg, H. Jürgensen, J. Selders, A. V. Solomonov, G. F. G. Linskii, and M. Razeghi, *J. Appl. Phys.* **54**, 4543 (1983).
- ¹⁵D. D. Sell and H. C. Casey, *J. Appl. Phys.* **45**, 800 (1974).
- ¹⁶W. J. Turner, W. E. Reese, and G. D. Pettit, *Phys. Rev.* **136**, A1467 (1964).
- ¹⁷W. C. Dash and R. Newman, *Phys. Rev.* **99**, 1151 (1955).
- ¹⁸V. P. Evtikhiev, D. Z. Garbuzov, and A. T. Gorelenok, *Fiz. Tekh. Poluprovodn.* **17**, 1402 (1983) [*Sov. Phys.—Semicond.* **17**, 891 (1983)].
- ¹⁹A. M. Fox, A. C. Maciel, J. F. Ryan, and M. D. Scott, *Appl. Phys. Lett.* **50**, 398 (1987).
- ²⁰Here $\Delta_0 \approx 0.35$ eV is the spin-orbit splitting energy; see, for example, Y. Yamazoe, T. Nishino, and Y. Hamakawa, *IEEE J. Quantum Electron.* **QE-17**, 139 (1981).